COVID-19 pandemic reveals persistent disparities in nitrogen dioxide pollution

Gaige Hunter Kerr[a,1] (ORCID), Daniel L. Goldberg[a,b] (ORCID), and Susan C. Anenberg[a] (ORCID)

[a]Department of Environmental and Occupational Health, Milken Institute School of Public Health, George Washington University, Washington, DC 20052; and [b]Energy Systems Division, Argonne National Laboratory, Lemont, IL 60439

The unequal spatial distribution of ambient nitrogen dioxide (NO_2), an air pollutant related to traffic, leads to higher exposure for minority and low socioeconomic status communities. We exploit the unprecedented drop in urban activity during the COVID-19 pandemic and use high-resolution, remotely sensed NO_2 observations to investigate disparities in NO_2 levels across different demographic subgroups in the United States. We show that, prior to the pandemic, satellite-observed NO_2 levels in the least White census tracts of the United States were nearly triple the NO_2 levels in the most White tracts. During the pandemic, the largest lockdown-related NO_2 reductions occurred in urban neighborhoods that have 2.0 times more non-White residents and 2.1 times more Hispanic residents than neighborhoods with the smallest reductions. NO_2 reductions were likely driven by the greater density of highways and interstates in these racially and ethnically diverse areas. Although the largest reductions occurred in marginalized areas, the effect of lockdowns on racial, ethnic, and socioeconomic NO_2 disparities was mixed and, for many cities, nonsignificant. For example, the least White tracts still experienced ∼1.5 times higher NO_2 levels during the lockdowns than the most White tracts experienced prior to the pandemic. Future policies aimed at eliminating pollution disparities will need to look beyond reducing emissions from only passenger traffic and also consider other collocated sources of emissions such as heavy-duty vehicles.

nitrogen dioxide | air pollution | environmental justice | COVID-19 | TROPOMI

Adverse air quality is an environmental justice issue, as it disproportionately affects marginalized and disenfranchised populations around the world (1–4). Growing evidence suggests that these populations experience more air pollution than is caused by their consumption (5–7). Within the United States, disparities in exposure are persistent, despite successful regulatory measures that have reduced pollution (8, 9). Nitrogen dioxide (NO_2) is a short-lived trace gas formed shortly after fossil fuel combustion and regulated by the National Ambient Air Quality Standards under the Clean Air Act. Exposure to NO_2 is associated with a range of respiratory diseases and premature mortality (10–12). NO_2 is also a precursor to other pollutants such as ozone and particulate matter (13). Major sources of anthropogenic NO_2, such as roadways and industrial facilities, are often located within or nearby marginalized and disenfranchised communities (14, 15), and disparities in NO_2 exposure across demographic subgroups have been the focus of several recent studies (4, 8, 16–18).

In early 2020, governments around the world imposed lockdowns and shelter-in-place orders in response to the spread of COVID-19. The earliest government-mandated lockdowns in the United States began in California on 19 March 2020, and many states followed suit in the following days. Changes in mobility patterns indicate that self-imposed social distancing practices were underway days to weeks before the formal announcement of lockdowns (19). Lockdowns led to sharp reductions in surface-level NO_2 (20–23) and tropospheric column NO_2 measured from satellite instruments (21, 24–27) over the United States, China, and Europe. According to government-reported inventories, roughly 60% of anthropogenic emissions of nitrogen oxides ($NO_x \equiv NO + NO_2$) in the United States in 2010 were emitted by on-road vehicles (28), and up to 80% of ambient NO_2 in urban areas can be linked to traffic emissions (29, 30). As such, NO_2 is often used as a marker for road traffic in urban areas. Multiple lines of evidence such as seismic quieting and reduced mobility via location-based services point to changes in traffic-related emissions as the main driver of reductions in NO_2 pollution during lockdowns, due to the large proportion of the population working from home (21, 23, 31, 32).

Here we exploit the unprecedented changes in human activity unique to the COVID-19 lockdowns and remotely sensed NO_2 columns with extraordinary spatial resolution and coverage to understand inequalities in the distribution of NO_2 pollution for different racial, ethnic, and socioeconomic subgroups in the United States. Specifically, we address the following: Which demographic subgroups received the largest NO_2 reductions? Did the lockdowns grow or shrink the perennial disparities in NO_2 pollution across different demographic subgroups? Although the lockdowns are economically unsustainable, how can they advance environmental justice and equity by informing long-term policies to reduce NO_2 disparities and the associated public health damages?

Results

Previous studies examining satellite-derived NO_2 found the highest levels in urban areas (33–35), and we find that these areas clearly stand out as NO_2 hotspots during our baseline period (Fig. 1A). NO_2 column densities averaged over all urban areas are ~ 2 times higher than over rural areas during the baseline period. Absolute differences in NO_2 between the baseline and lockdown periods ("drops") show sharp decreases over virtually all major metropolitan regions (Fig. 1B). The use of only spring 2019 for our baseline period stems from the short data record offered by the Tropospheric Monitoring Instrument (TROPOMI), and the slight increases in NO_2 in parts of the Great Plains and Midwest during lockdowns ($< 0.5 \times 10^{15}$ molecules per square centimeter) could reflect differences in natural (e.g., soil, lightning, stratospheric NO_x) or anthropogenic sources of NO_2 between the baseline and lockdown periods. Demetillo et al. (4) found that TROPOMI is capable of resolving NO_2 differences between census tracts in the Houston area, and our nationwide comparison of TROPOMI NO_2 with surface-level observations reveals TROPOMI's utility as a tool to understand NO_2 variability (SI Appendix, Text S1 and Fig. S1). The 3-mo baseline and lockdown periods used in this study have sufficient length to account for the influence of meteorological variability on NO_2, and NO_2 disparities found using a 3-mo period closely resemble disparities calculated with longer timeframes (SI Appendix, Fig. S2). Given that the largest lockdown-related changes in NO_2 occur in urban areas and to avoid urban–rural demographic gradients, we primarily focus on urban NO_2 changes and how these changes impact different demographic subgroups in urban areas.

The largest urban NO_2 drops occur in census tracts that are more non-White and Hispanic, have lower median household income, and have a higher proportion of their population without a vehicle or a postsecondary education compared with tracts with the smallest drops (Fig. 1 D–H). In tracts with the largest drops, there are ~ 2.0 times more non-White residents and ~ 2.1 times more Hispanic residents than in tracts with the smallest drops (Fig. 1 D and G). The differences in the "Other" category between tracts with largest and smallest drops (Fig. 1G) reflect differences in the Asian population (5% in tracts with the smallest drops; 14% in tracts with the largest drops) and the proportion of the population that does not identify as one of the census-designed racial categories (4% in tracts with smallest drops; 19% in tracts with the largest drops). These results for urban tracts also hold in all (urban and rural) tracts and rural tracts, despite the different demographic composition (compare Fig. 1 and SI Appendix, Fig. S3). Differences in distributions of demographic variables between tracts with the largest versus smallest drops in Fig. 1 C–H are all statistically significant.

Communities with lower income and educational attainment and a large proportion of racial and ethnic minorities have faced higher levels of NO_2 and other pollutants for decades (3, 8, 9, 16, 36), and we find that these communities experienced the largest drops in NO_2 pollution during COVID-19 lockdowns. However, Fig. 1 does not indicate how lockdown-related NO_2 drops grew
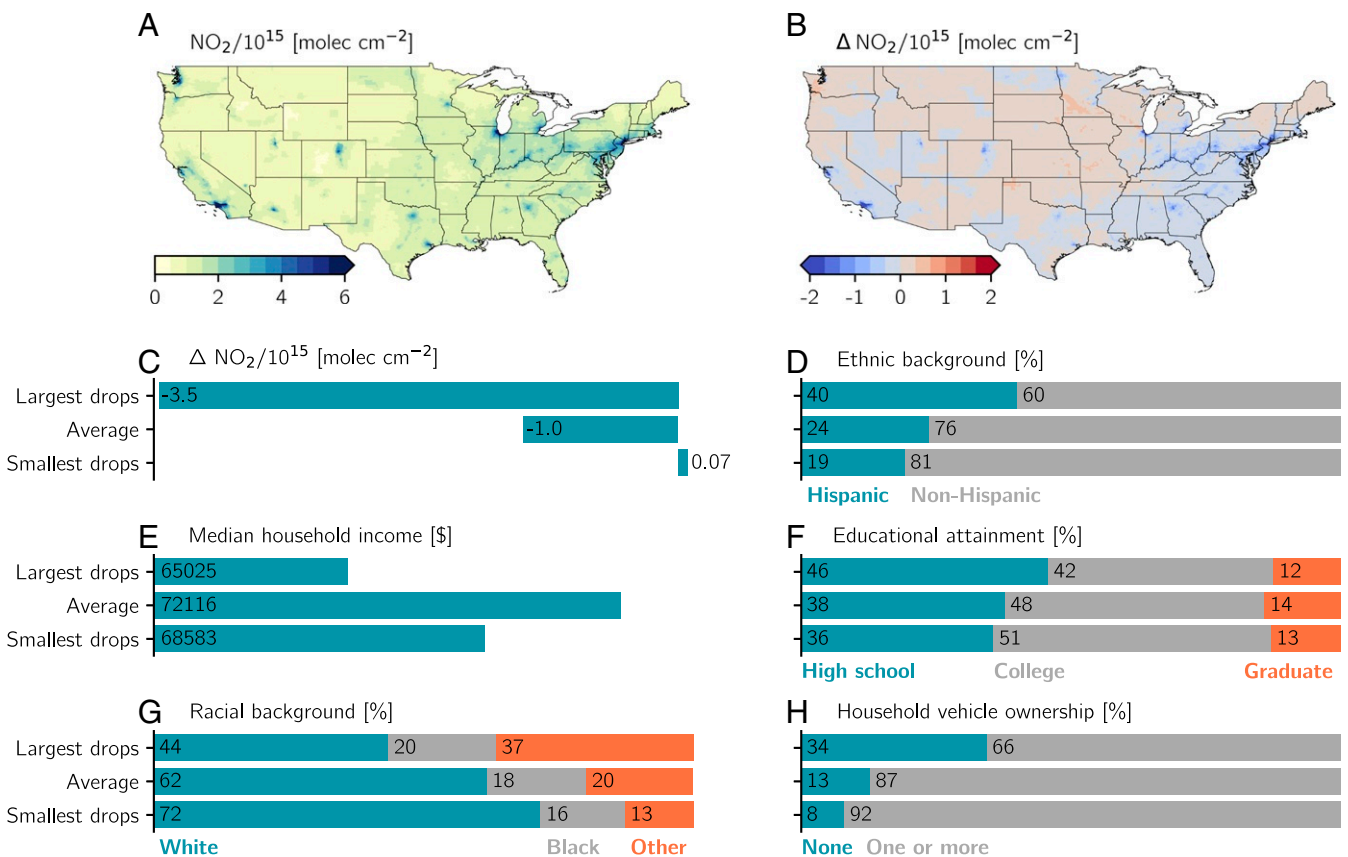
Fig. 1. Spatial distribution of NO_2 columns during the baseline and COVID-19 lockdown periods and apportionment of drops among different demographic subgroups. (A) Census tract average baseline NO_2 (13 March to 13 June 2019). (B) Absolute difference between lockdown (13 March to 13 June 2020) and baseline NO_2 (ΔNO_2), where $\Delta NO_2 < 0$ corresponds to NO_2 drops during lockdowns. (C–H) Demographic data averaged over urban tracts with the largest drops (ΔNO_2 in first decile), all urban tracts, and urban tracts with the smallest drops (ΔNO_2 in the tenth decile). "Other" in G includes American Indian or Alaska Native, Asian, Native Hawaiian or other Pacific Islander, two or more races, and some other race. The census-designated concept of race differs from ethnicity, and the percentage of White residents in G includes individuals with Hispanic origin or descent.

or shrunk disparities, and we next examine disparities in baseline and lockdown NO_2 in the most marginalized versus least marginalized census tracts in the United States.

In the baseline and lockdown periods, neighborhoods with lower income and educational attainment and those with a larger proportion of minority residents consistently face higher levels of NO_2 among all urban tracts across the United States and in nearly all of the 15 largest metropolitan statistical areas (MSAs) in the United States (Fig. 2 and *SI Appendix*, Fig. S4). There are some cases in which the most marginalized tracts do not experience the highest NO_2 levels. For example, rural tracts with the highest income and educational attainment have higher NO_2 levels than tracts with the lowest income or educational attainment (Fig. 2 *B* and *C*), and similar findings hold for specific MSAs (e.g., Riverside in Fig. 2*B*, Atlanta in Fig. 2*C*). Moreover, there are no significant differences in NO_2 distributions for tracts with the highest versus lowest income during the baseline period (Fig. 2*B*).

When considering all census tracts (both urban and rural), the most pronounced disparities, defined as the ratio of mean NO_2 for the marginalized subgroup to the nonmarginalized subgroup, are on the basis of race and ethnicity. The least White tracts and most Hispanic tracts have 2.6 and 2.2 times greater baseline NO_2 levels than the most White and least Hispanic tracts, respectively (Fig. 2*A* and *SI Appendix*, Figs. S4*A* and S5*G*). These disparities persist when examining individual MSAs in the United States. For example, baseline NO_2 in tracts with the lowest median household income in New York and Los Angeles is 1.4 and 1.8 times higher, respectively, than in tracts with the highest income (Fig. 2*B* and *SI Appendix*, Fig. S4*B*).

The unprecedented change in human activity during COVID-19 lockdowns led to mixed impacts on relative NO_2 disparities across different population subgroups, depending on the demographic variable and MSA considered (Fig. 2 and *SI Appendix*, Fig. S4). Racial NO_2 disparities for all census tracts significantly decreased from 2.6 to 2.0 during lockdowns, and a majority of the featured MSAs experienced significant reductions in their racial disparities (Fig. 2*A* and *SI Appendix*, Fig. S4*A*). Disparities for other demographic variables, however, were less affected by lockdowns. For example, a majority of MSAs had no significant reduction in disparities for different levels of income and educational attainment (Fig. 2 *B* and *C* and *SI Appendix*, Fig. S4 *B* and *C*). Understanding inconsistencies in the exact magnitude of NO_2 drops across MSAs for different population subgroups is beyond the scope of this study but could stem from varying stringencies of or adherence to lockdown measures.

Although urban areas experienced broad drops in NO_2 during lockdowns, with the largest drops occurring in marginalized neighborhoods (Fig. 1 *C–H*), NO_2 disparities in the baseline period were so large that even significant reductions in disparities did not generally bring lockdown NO_2 levels for marginalized neighborhoods to the levels experienced by nonmarginalized neighborhoods during the baseline period (Fig. 2). As an example, despite the unprecedented drop in human activity during the COVID-19 pandemic, NO_2 levels in the least White neighborhoods in New York and Chicago were $\sim 1 \times 10^{15}$ and $\sim 2 \times 10^{15}$ molecules per square centimeter higher, respectively, during lockdowns than levels in the most White neighborhoods during the baseline period. Houston, Washington, Philadelphia,
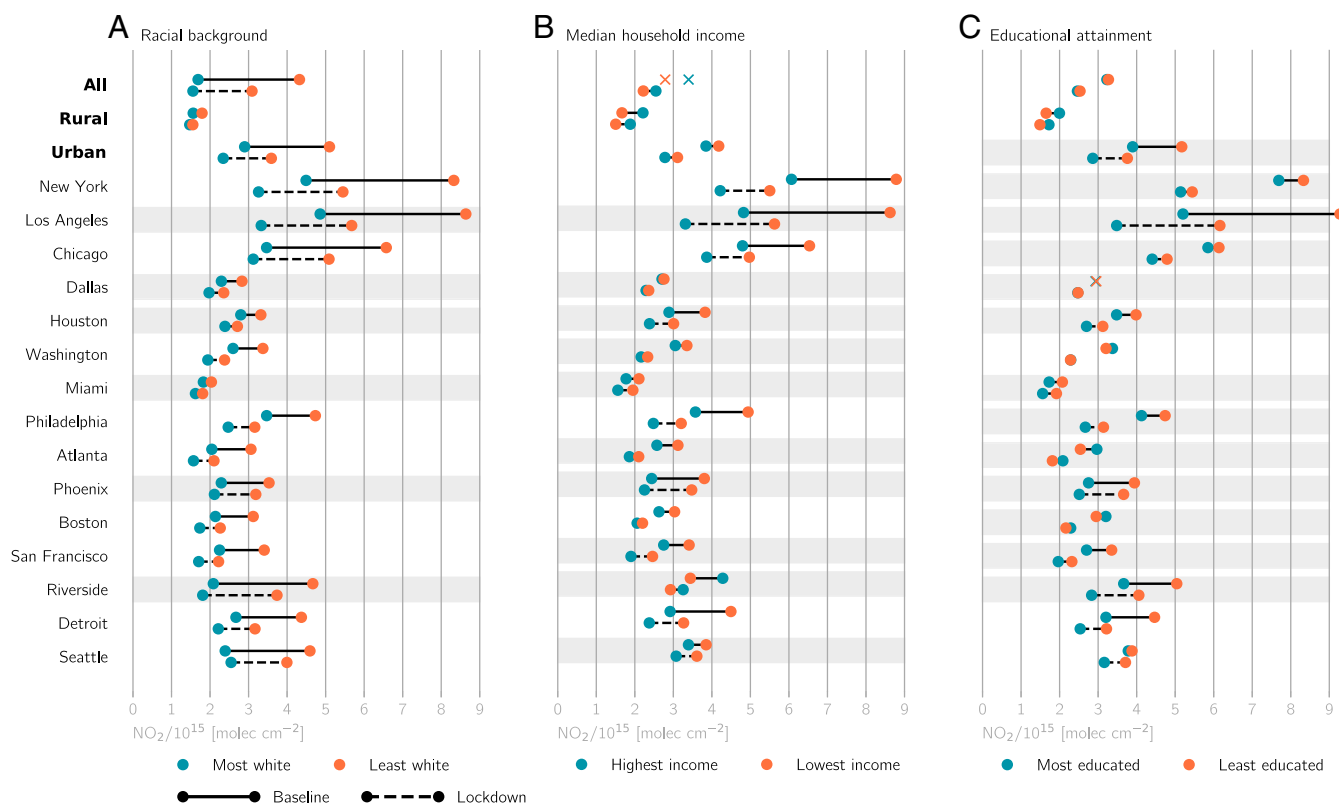
Fig. 2. Disparities in baseline and lockdown NO_2 columns for different (*A*) racial, (*B*) median household income, and (*C*) educational attainment population subgroups. Disparities are shown for three conglomerations (all, urban, and rural census tracts), and urban tracts are further separated into the 15 largest MSAs in the United States. For each conglomeration or MSA, demographic subgroups are determined using the 10th and 90th percentiles as thresholds. NO_2 levels are thereafter averaged over tracts within these subgroups. If the difference in subgroup NO_2 distributions for a particular demographic variable and time period is not statistically significant, mean NO_2 levels are denoted with an "X" and no connector lines. Conglomerations or MSAs with no significant change in NO_2 disparities between the baseline and lockdown periods are shaded in gray.

Kerr et al.
COVID-19 pandemic reveals persistent disparities in nitrogen dioxide pollution

PNAS | 3 of 8
https://doi.org/10.1073/pnas.2022409118

and San Francisco are notable exceptions to this result, and NO_2 levels for the least White tracts during lockdowns fell below NO_2 levels for the most White tracts during the baseline period in these cities. We observe similar results for population subgroups based on ethnicity, income, and educational attainment (Fig. 2 and *SI Appendix*, Figs. S4 and S5).

Within urban areas, we find that the magnitude of NO_2 drops is tightly coupled to the density of nearby primary roads (highways and interstates). The density of primary roads in urban tracts with the largest NO_2 drops (i.e., tracts in the first decile) is 9.5 times greater than in urban tracts with the smallest NO_2 drops (i.e., tenth decile) (Fig. 3). The racial, ethnic, income, and educational compositions of tracts are also closely related to primary road density. Urban tracts with lower income and vehicle ownership and a larger percentage of racial and ethnic minorities are located near a higher density of primary roads (Fig. 3). The difference in primary road density on the basis of vehicle ownership is especially stark: Tracts with the lowest vehicle ownership have a ~ 9.5 times higher primary road density than tracts with the highest ownership. Similarly, the least White tracts have a primary road density ~ 4.5 times higher than the most White tracts. Educational attainment is the only demographic variable considered in this study that exhibits a different relationship with primary road density, and we observe a U-shaped relationship between these variables (Fig. 3).

To better understand the impact of the lockdowns on NO_2 disparities, we consider case studies of individual cities: New York, Detroit, and Atlanta (Fig. 4). Among individual neighborhoods in each of these cities, the magnitude of NO_2 drops varies up to 50% above and below the citywide average (Fig. 4 *A–C*). The portions of New York, Atlanta, and Detroit that received the largest drops tend to have lower median household income and a high percentage of non-White residents (Fig. 4 *D–I*). Although the sharp decrease in passenger vehicle emissions (21, 23, 37) is the primary factor in explaining the large-scale NO_2 drops, examining drops on smaller neighborhood scales in New York, Atlanta, Detroit (Fig. 4), or other MSAs suggests that other sectors may contribute to the NO_2 drops, in addition to on-road activity. In New York, the largest drops are concentrated in Harlem and the South Bronx (Fig. 4*A*), where the high concentration of major highways and industrial facilities has been

linked to disproportionate exposure to air pollution (38). The largest drops in Atlanta occur in the southwestern part of the city, where median household income generally is $< \$30,000$ and the percentage of Black residents in each tract is nearly 100. Hartsfield-Jackson International Airport and several major highways are located in this part of Atlanta (Fig. 4*B*). The airport reported a $\sim 50\%$ decrease in the daily number of flights during lockdowns (39). Therefore, both on-road and aviation emissions may be responsible for the disparities in NO_2 levels in Atlanta. The largest drops in Detroit are concentrated on the west shores of the Detroit River; Interstates 75 and 94 and the Ambassador Bridge, one of the busiest US–Canada border crossings, transect this part of Detroit (Fig. 4*C*) (40). Although these Detroit neighborhoods are not predominantly non-White (Fig. 4*F*), they are home to a large Hispanic population with low median household income (Fig. 4*I*).

Discussion

Neighborhoods with a large proportion of racial and ethnic minorities, lower income, and lower educational attainment saw the greatest decreases in NO_2 pollution during the COVID-19 lockdowns. Although lockdowns were lauded as a temporary glimpse of the potential for cleaner urban air, NO_2 disparities persisted during this global natural experiment. For many cities, there were no significant changes in NO_2 disparities during the lockdowns, and marginalized communities faced higher NO_2 levels during the lockdowns than nonmarginalized communities experienced prior to the lockdowns. Our findings build on Demetillo et al. (4), who similarly used TROPOMI to understand environmental justice in Houston and inform drivers of inequality, and are consistent with contemporaneous studies that have analyzed long-term trends in NO_2 and other air pollutants and found that, despite widespread decreases in pollution, the most exposed demographic subgroups in the 1980s and 1990s remain the most exposed in the present day (8, 9).

Sources of urban NO_2 such as railroads, ports, airports, or industrial facilities are not disproportionately located in marginalized neighborhoods, do not contribute in a major way to total urban NO_x emissions, or were not largely affected by the pandemic (*SI Appendix*, Text S1 and Figs. S6–S8). The location of primary roads, however, is heavily skewed toward marginalized neighborhoods (Fig. 3), and on-road emissions from light- and heavy-duty vehicles represent a sizable contribution (~ 40 to 50%) to urban NO_x emissions (*SI Appendix*, Fig. S7). The collocation of primary roads with poor, minority communities is not happenstance but a consequence of the Eisenhower-era federal highway program, which often deliberately routed highways through these poor, minority neighborhoods (8, 15, 41, 42). While passenger vehicle traffic experienced a precipitous decline during the pandemic (21, 23, 37), heavy-duty trucking largely continued unabated (*SI Appendix*, Fig. S8). Together, these findings indicate that heavy-duty trucking plays a major role in explaining persistent disparities of NO_2 pollution among demographic subgroups. As was previously pointed out with the case studies of New York, Atlanta, and Detroit (Fig. 4), NO_2 sources beyond on-road transportation may be important to understand NO_2 disparities locally, but the small contribution of these other sources to total urban NO_x, their small or inconsistent changes during lockdowns, and their point source nature suggest that they are unlikely to explain the nationwide urban NO_2 disparities detailed herein.

Interestingly, urban tracts with the lowest vehicle ownership have both the highest density of nearby primary roads and the largest drops in NO_2 (Figs. 1*H* and 3). This result suggests that these communities may breathe more traffic-related NO_2 pollution than they produce. This is indeed the case for particulate matter pollution: Recent work found that particulate
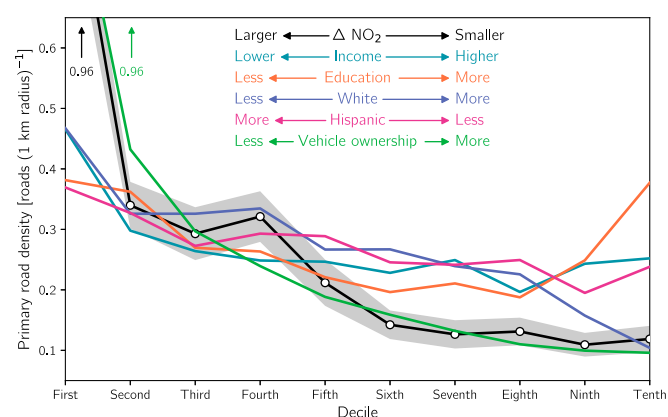
Fig. 3. The relationship of road density with urban lockdown-related drops in NO_2 columns and demographic variables. Road density is calculated as the number of primary road segments within a 1-km radius of tracts' centroids for each decile of demographic variables. The colored legend indicates the directionality of each demographic variable. As an example, the density corresponding to the lowest decile of the "White" curve represents the road density in urban tracts that are the least White (i.e., in the first decile of the percentage of their population that is White). Shading for the ΔNO_2 curve illustrate the 90% CI.

Fig. 4. Case studies of lockdown NO_2 drops, income, and race for (*A, D,* and *G*) New York, (*B, E,* and *H*) Atlanta, and (*C, F,* a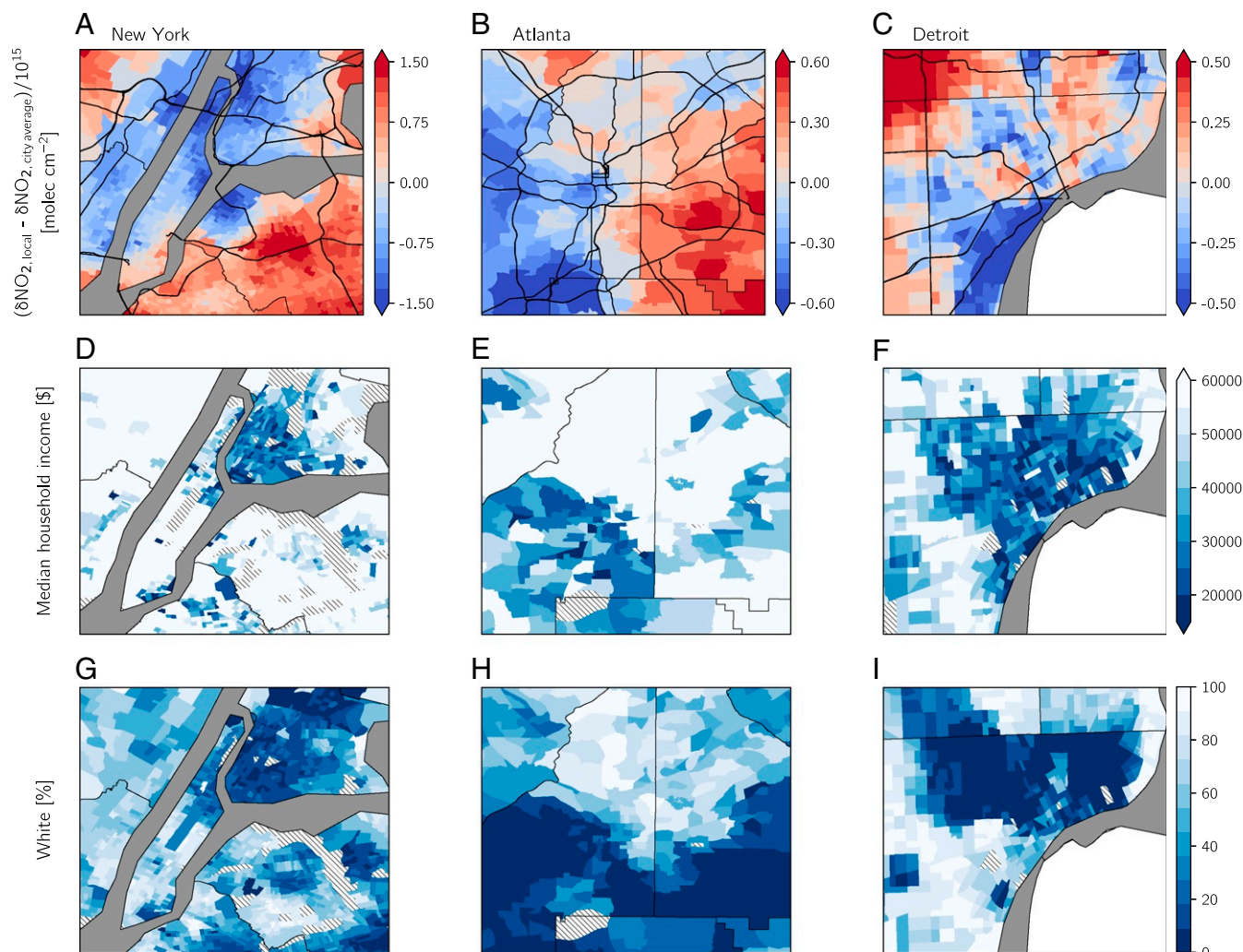nd *I*) Detroit. (*A–C*) $\triangle\ NO_{2,\,local}$ is calculated from oversampled TROPOMI data as the difference between $\triangle\ NO_2$ and the city average $\triangle\ NO_2$ to highlight neighborhoods with larger drops (i.e., negative values) and smaller drops (i.e., positive values) compared with the city-averaged drops. Primary roads are shown in thick black lines. (*D–F*) Median household income and (*G–I*) percentage of the population that is White. Tracts in *D–I* that are employment centers, airports, parks, or forests and therefore report no demographic data are denoted with hatching.

matter exposure is disproportionately caused by wealthy, non-Hispanic White communities, while poor, Black, and Hispanic communities face higher exposure than is caused by their own consumption (6, 7).

Preliminary research suggests that high levels of NO_2 pollution contribute to underlying health conditions that lead to increased COVID-19 fatality rates (43). Therefore, the decrease in NO_2 in diverse communities with low income or educational attainment could decrease population susceptibility to COVID-19. This result is especially important as these communities have increased risk for COVID-19 and higher hospitalization rates (44). Since short-term NO_2 exposure is associated with respiratory disease (45, 46), the temporary NO_2 drops may have also reduced acute respiratory health outcomes, but the actual health effects of NO_2 drops during the pandemic are difficult to tease out since the degree to which people sought health care was also affected by the pandemic. These findings are especially relevant for marginalized neighborhoods in cities (e.g., New York, Atlanta, and Detroit; Fig. 4) that have been long plagued by high rates of asthma and other respiratory diseases due, in part, to their proximity to on-road and point source NO_x emissions (38, 40).

We have considered singular demographic variables and their relationship with baseline and lockdown NO_2. The case studies in Fig. 4 hint that the intersectionality between race and poverty may be associated with even more pronounced lockdown-related drops in NO_2 pollution. Although the vast majority of tracts in the southern half of Atlanta have a majority non-White population (Fig. 4*H*), the largest drops occur in tracts that are both majority non-White and low income (Fig. 4 *B, E,* and *H*). Clark et al. (17) and Demetillo et al. (4) examined NO_2 exposure in neighborhoods where poverty and racial and ethnic identities intersect and found a disproportionate share of NO_2 pollution for neighborhoods with these intersecting identities. Assessing other forms of intersectionality and their relationship with air pollution exposure is a key area for future research.

Recent work demonstrates that satellite-observed NO_2 is a powerful proxy for ground-level NO_2 gradients (47), and TROPOMI, in particular, provides significant advances over predecessor instruments, on account of its unprecedented spatial resolution (48). We tested whether TROPOMI has consistent spatial patterns with surface-level observations during the baseline period and found good agreement (*SI Appendix*, Fig. S1A). TROPOMI's correlation with surface-level monitors (*SI*

Kerr et al.
COVID-19 pandemic reveals persistent disparities in nitrogen dioxide pollution

PNAS | 5 of 8
https://doi.org/10.1073/pnas.2022409118

Appendix, Text S1 and Fig. S1*A*) is a dramatic improvement over predecessor instruments (49). Moreover, the ratios of 24-h average NO_2 to NO_2 near the time of satellite overpass are also similar between least and most polluted sites (*SI Appendix*, Fig. S1*B*). We note, however, that satellite-derived NO_2 tends to underestimate NO_2 in highly polluted urban regions, on account of satellite footprint resolution (50). This underestimation, coupled with the fact that marginalized communities tend to live closer to potent NO_2 sources such as highways (Fig. 3) that cannot be resolved given TROPOMI's resolution, suggests that our current methodology may underestimate the magnitude of disparities and lockdown-related changes.

Our results are neither an artifact of how we defined demographic subgroups (*SI Appendix*, Fig. S5) nor the time period over which we characterize disparities, although the precise absolute NO_2 levels and magnitude of disparities change with the start dates and length of the periods (*SI Appendix*, Figs. S2 and S9). We encourage future work using surface-level NO_2 concentrations to better understand exposure across demographic subgroups during lockdowns. Current surface-level observational networks are inadequate for doing so, due to their sparse and uneven distribution (51), but surface concentrations of NO_2 observed from networks of low-cost sensors (52) or inferred using land-use regression models (53) and chemical transport models (34, 54) may prove useful. Future work might also examine how lockdown-related changes in other air pollutants such as ozone and particulate matter, whose changes during lockdowns do not exhibit the same spatial patterns as NO_2 (22, 23, 55), impact disparities.

Conclusions

This study provides a unique look at air pollution disparities in the United States, leveraging the confluence of unparalleled changes in human activity during COVID-19 lockdowns and the unmatched spatial coverage and resolution of air quality surveillance from the TROPOMI satellite instrument. Lockdowns decreased tropospheric column abundances of NO_2 across the vast majority of urban areas. However, drops in NO_2 pollution were uneven within these urban areas, and the largest drops occurred in communities with a high proportion of racial and ethnic minorities and lower educational attainment and income. Our results reveal that, despite the decreases in NO_2 pollution during lockdowns, racial, ethnic, and socioeconomic NO_2 disparities persisted, and marginalized communities continued to face higher levels of NO_2 during the lockdowns than nonmarginalized communities experienced prior to the pandemic. As passenger vehicles represent a large source of urban NO_x emissions, the proximity of marginalized neighborhoods to a high density of major roadways is likely the key determinant in explaining lockdown-related drops in NO_2.

Our results offer insight into policies aimed at reducing or eliminating ethnoracial and socioeconomic NO_2 disparities. The COVID-19 lockdowns showed that a dramatic drop in NO_x emissions mainly from the passenger vehicle sector narrowed NO_2 disparities only modestly and not consistently across major US cities. Heavy-duty diesel vehicles, on the other hand, maintained more or less the same activity levels during the COVID-19 lockdowns, continue to be a major contributor to urban NO_x emissions, and use highways and interstates disproportionately located in marginalized communities. While decreasing NO_x emissions from passenger vehicles, airports, railways, ports, and industry would broadly reduce NO_2 levels and is relevant for disparities in some cities, targeting NO_x emissions from heavy-duty diesel vehicles is likely the most effective strategy for reducing disparities across cities nationwide. Future studies and policy strategies should therefore examine how targeting heavy-duty diesel traffic can address inequity in exposure while maximizing health benefits.

Materials and Methods

Remotely Sensed NO₂. We obtain retrievals of the tropospheric NO_2 column from the TROPOMI aboard the Sentinel-5 Precursor (S5P) satellite. S5P is a nadir-viewing satellite in a sun-synchronous, low-Earth orbit that achieves near-global daily coverage with a local overpass time of $\sim 1,330$ h (56). TROPOMI provides NO_2 measurements at an unprecedented spatial resolution of 5×3.5 km (7×3.5 km prior to 6 August 2019) (57). We use level 2 data and only consider pixels with a quality assurance value of > 0.75. The change in satellite resolution occurring in August 2019 as well as intrinsic limitations stemming from the retrieval process and satellite footprint likely lead to an underestimation of NO_2 levels in urban areas and potentially the NO_2 change during lockdowns (47, 50). TROPOMI data are thereafter oversampled by regridding to a standard grid with a resolution of $0.01°$ latitude $\times 0.01°$ longitude ($\sim 1 \times 1$ km) and averaged over two time periods: a baseline period (13 March to 13 June 2019) and a lockdown period (13 March to 13 June 2020). Regridded data are publicly available at Figshare (https://figshare.com/s/75a00608f3faedc4bca7).

Comparing the same time period across different years is commonplace in satellite studies investigating changes in NO_x and other trace gases, and averaging over 3-mo timeframes smooths natural NO_2 variations that arise from differences in meteorology and sun angle, which are especially relevant during boreal spring (26) (*SI Appendix*, Fig. S2). This temporal averaging also removes most of the random error in the TROPOMI single-pixel uncertainties, which can be 40 to 60% of the tropospheric column abundances (24).

Sociodemographic Data. Demographic information is derived from the American Community Survey (ACS) conducted by the US Census Bureau and maintained by the National Historical Geographic Information System (58). Data are publicly available at https://www.nhgis.org. We extract 2014–2018 5-y estimates on race, Hispanic or Latino origin (henceforth "ethnicity"), educational attainment, median household income, and vehicle availability for the 72,538 census tracts in the contiguous United States. To minimize the number of different categorical variables presented in this study, we combine racial groups into three categories: White, Black (includes Black and African American), and Other (includes American Indian or Alaska Native, Asian, Native Hawaiian or Other Pacific Islander, two or more races, and some other race). Similarly, we form three different levels for educational attainment: high school (includes no high school diploma, regular high school diploma, and GED or alternative credentials), college (includes some college without a degree, associate's degree, and bachelor's degree), and graduate (includes master's degree, professional school degree, and doctorate degree).

Methods We harmonize the regridded TROPOMI NO_2 measurements with tract-level ACS demographics by determining the geographic boundaries of each tract and thereafter calculating a simple arithmetic average over all TROPOMI grid cells within the tract for the baseline and lockdown periods. While the area of most census tracts is much larger than the $\sim 1 \times 1$ km TROPOMI grid cells (*SI Appendix*, Fig. S10), approximately 8% of tracts lack a colocated grid cell, due to their small size (or irregular geometry). For example, the median area of census tracts in New York is 0.7 km² (*SI Appendix*, Fig. S10). For these small tracts, we employ inverse distance weighting interpolation to calculate the NO_2 levels at their centroids using NO_2 levels in the eight neighboring grid cells. This approach may smooth over the fine-scale NO_2 gradients present in very small tracts and potentially underestimate the impacts of NO_x emissions (4). Tracts are classified as either rural or urban based on the census-designed rurality level from the last decadal census in 2010. Urban census tracts lie within the boundaries of an incorporated or census-designed place with $> 2,500$ residents, and rural tracts are located outside these boundaries. Therefore, suburban areas on the periphery of cities with $> 2,500$ residents are classified as "urban" in this study. We further stratify the tracts into metropolitan-level subsets for the 15 largest MSAs in the United States: New York City–Newark–Jersey City, NY–NJ–PA; Los Angeles–Long Beach–Anaheim, CA; Chicago–Naperville–Elgin, IL–IN–WI; Dallas–Fort Worth–Arlington, TX; Houston–The Woodlands–Sugar Land, TX; Washington–Arlington–Alexandria, DC–VA–MD–WV; Miami–Fort Lauderdale–Pompano Beach, FL; Philadelphia–Camden–Wilmington, PA–NJ–DE–MD; Atlanta–Sandy Springs–Alpharetta, GA; Phoenix–Mesa–Chandler, AZ; Boston–Cambridge–Newton, MA–NH; San Francisco–Oakland–Berkeley, CA; Riverside–San Bernardino–Ontario, CA; Detroit–Warren–Dearborn, MI; and Seattle–Tacoma–Bellevue, WA. For brevity, we refer to these MSAs by their colloquial names (e.g., Los Angeles, rather than Los Angeles–Long Beach–Anaheim, CA) when discussing them.

We calculate the density of nearby primary roadways for each census tract as a proxy for exposure to traffic-related NO_2 pollution. Primary roads are generally divided, limited-access highways within the Interstate Highway System or under state management, and their locations are determined from the US Census Bureau's TIGER/Line geospatial database. Specifically, we determine density as the number of primary road segments within 1 km of a tract's centroid. We choose 1 km as our threshold for "nearby," as NO_2 concentrations decrease up to $\sim 50\%$ within 0.5 km to 2 km from major roadways (4, 53). Other means of quantifying traffic exist (e.g., length of roadway within a specified distance, traffic within buffer zones, sum of distance traveled) (59), but our approach allows for consistent use of geospatial data from the US Census Bureau.

We partition census tracts by extreme values of their change in NO_2 ($\triangle NO_2$) or demographic variables using the first decile (0 to 10th percentile) and tenth decile (90th to 100th percentile). As examples, tracts classified as "most White" or "highest income" have a White population fraction or median household income which falls in the tenth decile. Similarly, $\triangle NO_2$ in tracts with the "largest drops" (i.e., the largest decrease in NO_2 during lockdowns) falls in the first decile. Decile thresholds are defined separately for all, urban, and rural census tracts and for different MSAs to account for urban–rural gradients and differences among MSAs. We note that, when this approach is applied to all (urban and rural) census tracts, a broad distribution of tracts is selected, not just tracts from a certain geographic region; for example, the $\sim$7,200 tracts classified as "most White" for all urban and rural census tracts represent tracts from all 48 states in the contiguous United States and Washington, DC. Our results are not sensitive to the use of the first and tenth deciles, and we have tested the upper and lower vigintiles, quintiles, and quartiles and obtained similar results (SI Appendix, Fig. S5). The use of percentiles rather than absolute thresholds yields a consistent sample size for the upper and lower extrema and also avoids defining absolute thresholds for different variables.

We applied the two-sample Kolmogorov–Smirnov (KS) test to determine whether distributions of demographic variables in tracts with the largest

and smallest NO_2 drops (Fig. 1 C–H) and tract-averaged NO_2 for the upper and lower extrema of demographic variables (Fig. 2) are drawn from the same distribution (SI Appendix, Fig. S11). If the p value corresponding to the KS test statistic is less than $\alpha = 0.05$, we declare that there are significant differences in the distributions. We also assess whether the NO_2 disparities shown in Fig. 2 undergo significant changes between the baseline and lockdown periods, using a two-sample z test. To meet the normality assumption of the z test, we log-transform the skewed NO_2 distributions prior to computing the test statistic. Changes in baseline versus lockdown disparities are classified as significant when the absolute value of the test statistic is larger than 1.96, the critical value for a 95% level of confidence ($p < 0.05$). We note that this approach to assess the significance of changes in disparities agrees well with other methods, such as examining whether 95% confidence levels of the baseline and lockdown disparities overlap (compare Fig. 2 and SI Appendix, Fig. S4).

The start date of the baseline and lockdowns periods used in this study (13 March) corresponds to the date of national emergency declaration in the United States and the beginning of a pronounced decrease in mobility patterns in 2020 (19). We test whether the overall racial, ethnic, income, and educational disparities hold for other periods and find that the disparities among different demographic subgroups persist regardless of the start date or length of the baseline period (SI Appendix, Figs. S2 and S9). We are inherently limited by the short TROPOMI data record, and interannual variability could play a role in modulating the magnitude of disparities in NO_2 levels. Testing this possibility is important as more TROPOMI data become available.

1. M. L. Bell, K. Ebisu, Environmental inequality in exposures to airborne particulate matter components in the United States. *Environ. Health Perspect.* **120**, 1699–1704 (2012).
2. P. J. Landrigan *et al.*, The Lancet Commission on pollution and health. *Lancet* **391**, 462–512 (2018).
3. C. J. Schell *et al.*, The ecological and evolutionary consequences of systemic racism in urban environments. *Science* **369**, eaay4497 (2020).
4. M. A. G. Demetillo *et al.*, Observing nitrogen dioxide air pollution inequality using high-spatial-resolution remote sensing measurements in houston, Texas. *Environ. Sci. Technol.* **54**, 9882–9895 (2020).
5. N. P. Nguyen, J. D. Marshall, Impact, efficiency, inequality, and injustice of urban air pollution: Variability by emission location. *Environ. Res. Lett.* **13**, 024002 (2018).
6. C. W. Tessum *et al.*, Inequity in consumption of goods and services adds to racial–ethnic disparities in air pollution exposure. *Proc. Natl. Acad. Sci. U.S.A.* **116**, 6001–6006 (2019).
7. B. Sergi, I. Azevedo, S. J. Davis, N. Z. Muller, Regional and county flows of particulate matter damage in the US. *Environ. Res. Lett.* **15**, 104073 (2020).
8. L. P. Clark, D. B. Millet, J. D. Marshall, Changes in transportation-related air pollution exposures by race-ethnicity and socioeconomic status: Outdoor nitrogen dioxide in the United States in 2000 and 2010. *Environ. Health Perspect.* **125**, 097012 (2017).
9. J. Colmer, I. Hardman, J. Shimshack, J. Voorhies, Disparities in $PM_{2.5}$ air pollution in the United States. *Science* **369**, 575–578 (2020).
10. M. Jerrett *et al.*, Spatial analysis of air pollution and mortality in California. *Am. J. Respir. Crit. Care Med.* **188**, 593–599 (2013).
11. S. C. Anenberg *et al.*, Estimates of the global burden of ambient $PM_{2.5}$, ozone, and NO_2 on asthma incidence and emergency room visits. *Environ. Health Perspect.* **126**, 107004 (2018).
12. P. Achakulwisut, M. Brauer, P. Hystad, S. C. Anenberg, Global, national, and urban burdens of paediatric asthma incidence attributable to ambient NO_2 pollution: Estimates from global datasets. *Lancet Planet. Health* **3**, e166–e178 (2019).
13. A. Stohl *et al.*, Evaluating the climate and air quality impacts of short-lived pollutants. *Atmos. Chem. Phys.* **15**, 10529–10566 (2015).
14. P. Mohai, P. M. Lantz, J. Morenoff, J. S. House, R. P. Mero, Racial and socioeconomic disparities in residential proximity to polluting industrial facilities: Evidence from the Americans' Changing Lives Study. *Am. J. Publ. Health* **99**, S649–S656 (2009).
15. G. M. Rowangould, A census of the US near-roadway population: Public health and environmental justice considerations. *Transport. Res. Transport Environ.* **25**, 59–67 (2013).
16. A. Hajat *et al.*, Air pollution and individual and neighborhood socioeconomic status: Evidence from the Multi-Ethnic Study of Atherosclerosis (MESA). *Environ. Health Perspect.* **121**, 1325–1333 (2013).
17. L. P. Clark, D. B. Millet, J. D. Marshall, National patterns in environmental injustice and inequality: Outdoor NO_2 air pollution in the United States. *PLoS One* **9**, e94431 (2014).
18. J. I. Levy, A. M. Wilson, L. M. Zwack, Quantifying the efficiency and equity implications of power plant air pollution control strategies in the United States. *Environ. Health Perspect.* **115**, 743–750 (2007).
19. H. S. Badr *et al.*, Association between mobility patterns and COVID-19 transmission in the USA: A mathematical modelling study. *Lancet Infect. Dis.* **20**, 1247–1254 (2020).
20. G. He, Y. Pan, T. Tanaka, The short-term impacts of COVID-19 lockdown on urban air pollution in China. *Nat. Sustainability* **3**, 1005–1011 (2020).
21. H. A. Parker, S. Hasheminassab, J. D. Crounse, C. M. Roehl, P. O. Wennberg, Impacts of traffic reductions associated with COVID-19 on southern California air quality. *Geophys. Res. Lett.* **47**, e2020GL090164 (2020).
22. X. Shi, G. P. Brasseur, The response in air quality to the reduction of Chinese economic activities during the COVID-19 outbreak. *Geophys. Res. Lett.* **47**, e2020GL088070 (2020).
23. Z. S. Venter, K. Aunan, S. Chowdhury, J. Lelieveld, COVID-19 lockdowns cause global air pollution declines. *Proc. Natl. Acad. Sci. U.S.A.* **117**, 18984–18990 (2020).
24. M. Bauwens *et al.*, Impact of coronavirus outbreak on NO_2 pollution assessed using TROPOMI and OMI observations. *Geophys. Res. Lett.* **47**, e2020GL087978 (2020).
25. J. Ding *et al.*, NO_x emissions reduction and rebound in China due to the COVID-19 crisis. *Geophys. Res. Lett.* **47**, e2020GL089912 (2020).
26. D. L. Goldberg *et al.*, Disentangling the impact of the COVID-19 lockdowns on urban NO_2 from natural variability. *Geophys. Res. Lett.* **47**, e2020GL089269 (2020).
27. K. Miyazaki *et al.*, Air quality response in China linked to the 2019 novel coronavirus (COVID-19) lockdown. *Geophys. Res. Lett.* **47**, e2020GL089252 (2020).
28. US Environmental Protection Agency, 2014 National Emissions Inventory (NEI) data. https://www.epa.gov/air-emissions-inventories/2014-national-emissions-inventory-nei-data. Accessed 15 October 2020.
29. I. Levy, C. Mihele, G. Lu, J. Narayan, J. R. Brook, Evaluating multipollutant exposure and urban air quality: Pollutant interrelationships, neighborhood variability, and nitrogen dioxide as a proxy pollutant. *Environ. Health Perspect.* **122**, 65–72 (2014).
30. I. Sundvor *et al.*, "Road traffic's contribution to air quality in European cities" (Tech. Rep. 2012/14, European Topic Centre for Air Pollution and Climate Change Mitigation, 2013).
31. N. S. Diffenbaugh *et al.*, The COVID-19 lockdowns: A window into the earth system. *Nat. Rev. Earth Environ.* **1**, 470–481 (2020).
32. T. Lecocq *et al.*, Global quieting of high-frequency seismic noise due to COVID-19 pandemic lockdown measures. *Science* **369**, 1338–1343 (2020).
33. N. A. Krotkov *et al.*, Aura OMI observations of regional SO_2 and NO_2 pollution changes from 2005 to 2015. *Atmos. Chem. Phys.* **16**, 4605–4629 (2016).
34. M. J. Cooper, R. V. Martin, C. A. McLinden, J. R. Brook, Inferring ground-level nitrogen dioxide concentrations at fine spatial resolution applied to the TROPOMI satellite instrument. *Environ. Res. Lett.* **15**, 104013 (2020).
35. D. L. Goldberg *et al.*, TROPOMI NO_2 in the United States: A detailed look at the annual averages, weekly cycles, effects of temperature, and correlation with surface NO_2 concentrations *Earth Future* **9**, e2020EF001665 (2021).

Kerr et al.
COVID-19 pandemic reveals persistent disparities in nitrogen dioxide pollution

PNAS | 7 of 8
https://doi.org/10.1073/pnas.2022409118

36. A. Hajat, C. Hsia, M. S. O'Neill, Socioeconomic disparities and air pollution exposure: A global review. *Curr. Environ. Health Rep.* **2**, 440–450 (2015).

37. C. L. Quéré *et al.*, Temporary reduction in daily global CO_2 emissions during the COVID-19 forced confinement. *Nat. Clim. Change* **10**, 647–653 (2020).

38. M. M. Patel *et al.*, Spatial and temporal variations in traffic-related particulate matter at New York City high schools. *Atmos. Environ.* **43**, 4975–4981 (2009).

39. K. Shah, 'Mostly empty': COVID-19 has nearly shut down world's busiest airport. *The Guardian*, 13 April 2020. https://www.theguardian.com/world/2020/apr/13/atlanta-hartsfield-jackson-coronavirus-airport-shut-down. Accessed 15 October 2020.

40. S. Martenies, C. Milando, G. Williams, S. Batterman, Disease and health inequalities attributable to air pollutant exposure in Detroit, Michigan. *Int. J. Environ. Res. Publ. Health* **14**, 1243 (2017).

41. M. H. Rose, R. A. Mohl, *Interstate: Highway Politics and Policy since 1939* (The University of Tennessee Press, Knoxville, TN, ed. 3, 2012).

42. T. K. Boehmer, S. L. Foster, J. R. Henry, E. L. Woghiren-Akinnifesi, F. Y. Yip, Residential proximity to major highways - United States, 2010. *Morb. Mortal. Wkly. Rep.* **62**, 46–50 (2013).

43. D. Liang *et al.*, Urban air pollution may enhance COVID-19 case-fatality and mortality rates in the United States. *Innovation* **1**, 100047 (2020).

44. M. A. Raifman, J. R. Raifman, Disparities in the population at risk of severe illness from COVID-19 by race/ethnicity and income. *Am. J. Prev. Med.* **59**, 137–139 (2020).

45. A. Chauhan *et al.*, Personal exposure to nitrogen dioxide (NO_2) and the severity of virus-induced asthma in children. *Lancet* **361**, 1939–1944 (2003).

46. N. N. Hansel, M. C. McCormack, V. Kim, The effects of air pollution and temperature on COPD. *COPD* **13**, 372–379 (2015).

47. M. J. Bechle, D. B. Millet, J. D. Marshall, Remote sensing of exposure to NO_2: Satellite versus ground-based measurement in a large urban area. *Atmos. Environ.* **69**, 345–353 (2013).

48. D. L. Goldberg *et al.*, Enhanced capabilities of TROPOMI NO_2: Estimating NO_x from North American cities and power plants. *Environ. Sci. Technol.* **53**, 12594–12601 (2019).

49. D. L. Goldberg *et al.*, A high-resolution and observationally constrained OMI NO_2 satellite retrieval. *Atmos. Chem. Phys.* **17**, 11403–11421 (2017).

50. L. M. Judd *et al.*, Evaluating the impact of spatial resolution on tropospheric NO_2 column comparisons within urban areas using high-resolution airborne data. *Atmos. Meas. Tech.* **12**, 6091–6111 (2019).

51. L. N. Lamsal *et al.*, U.S. NO_2 trends (2005-2013): EPA Air Quality System (AQS) data versus improved observations from the Ozone Monitoring Instrument (OMI). *Atmos. Environ.* **110**, 130–143 (2015).

52. K. Do *et al.*, A data-driven approach for characterizing community scale air pollution exposure disparities in inland Southern California. *J. Aerosol Sci.* **152**, 105704 (2021).

53. E. V. Novotny, M. J. Bechle, D. B. Millet, J. D. Marshall, National satellite-based land-use regression: NO_2 in the United States. *Environ. Sci. Technol.* **45**, 4407–4414 (2011).

54. J. A. Geddes, R. V. Martin, B. L. Boys, A. van Donkelaar, Long-term trends worldwide in ambient NO_2 concentrations inferred from satellite observations. *Environ. Health Perspect.* **124**, 281–289 (2016).

55. Y. Chang *et al.*, Puzzling haze events in China during the coronavirus (COVID-19) shutdown. *Geophys. Res. Lett.* **47**, e2020GL088533. (2020).

56. J. Veefkind *et al.*, TROPOMI on the ESA Sentinel-5 Precursor: A GMES mission for global observations of the atmospheric composition for climate, air quality and ozone layer applications. *Rem. Sens. Environ.* **120**, 70–83 (2012).

57. J. van Geffen *et al.*, S5P TROPOMI NO_2 slant column retrieval: Method, stability, uncertainties and comparisons with OMI. *Atmos. Meas. Tech.* **13**, 1315–1335 (2020).

58. S. Manson, J. Schroeder, D. V. Riper, S. Ruggles, IPUMS National historical geographic information system: Version 14.0 (IPUMS, Minneapolis, MN, 2019). http://doi.org/10.18128/D050.V14.0. Accessed 18 August 2020.

59. G. C. Pratt *et al.*, Quantifying traffic exposure. *J. Expo. Sci. Environ. Epidemiol.* **24**, 290–296 (2013).